Linear Model Predictive Control of Small-Scale Furnaces

M. Fallmann, L. Böhler & M. Kozek
TU Wien, Vienna, Austria

ABSTRACT: A comprehensive linear model predictive control framework for small-scale furnaces is introduced. Its formulation allows to meet restrictive legal emission regulations by utilizing a carbon monoxide formation model and provides a simple model-based approach to handle fuel switches efficiently. Experimental results confirm emission limiting behavior and robustness in the presence of fuel switches as well as changes of the operating point. Proposed methods stand out by their simplicity allowing for its use even in small and cost-driven applications. This paper covers topics published in (Böhler et al. 2020b) and extends them with additional measurement results and suggestions for a control redesign from scratch.

1. INTRODUCTION

Especially in the face of climate change, sustainability of biomass combustion motivates its ongoing research and development. Although highly sophisticated methods dictate hardware design, combustion control largely remains on the level of standard PID approaches (Kaltschmidt et al. 2016).

However, current and in particular upcoming legal emission regulations call for control algorithms being able to increase efficiency while maintaining robustness and simplicity of current methods. Model predictive controllers (MPCs) satisfy these requirements and have already been used for combustion control. Despite some successful implementations in large furnaces, see e.g. Kortela & Jämsä-Jounela (2014), their complexity inhibited broad application for small-scale units up to now. Therefore, this paper suggests a simple and purely linear model predictive control approach. Besides its overall simplicity, the ability to handle fuel switches in a highly efficient way stands out and has not been covered in related works.

In terms of emission limiting control, published approaches either lack of appropriate formation models, see e.g. Korpela et al. (2009), or utilize highly complex emission models needing time-consuming identification procedures (Peng et al. 2004). By contrast, this work relies on a static nonlinear formation model, proposed in literature (Böhler et al. 2019), and interlaces its findings into furnace control by methodically chosen reference values. The resulting emission limiting controller is characterized by its efficiency and flexibility and can be easily adapted to other furnaces.

2. FURNACE MODEL

The investigated small-scale biomass grate furnace, see a schematic drawing in Fig. 1, is mainly designed for the combustion of wooden pellets and thereby possesses a nominal heat output of 100 kW. While the fuel mass flow $\dot{m}_{fuel}$ is fed onto the grate, the primary and secondary air mass flows, $\dot{m}_{pa}$ and $\dot{m}_{sa}$, allow for its oxidation. Secondary air supply carried out in a spatially partitioned manner ($\dot{m}_{sa} = \dot{m}_{sa,1} + \dot{m}_{sa,2}$) facilitates mixing of inlet air and partially oxidized gases, therefore increasing combustion quality. Subsequently, the flue gas mass flow $\dot{m}_{fg}$ leaves the combustion chamber with the freeboard temperature T_{fb} and passes through the gas/water heat exchanger before it is finally released into the atmosphere with the reduced flue gas temperature T_{fg}. Without loss of general applicability of the concept presented hereinafter, the return temperature T_{ret} and water mass flow $\dot{m}_w$ are kept constant in the experimental setup. Since relevant heat output is therefore directly proportional to the supply temperature T_{sup}, major importance of this physical quantity in the given investigation is further emphasized.

The lumped model utilized within this work is based on simple analytic approaches, discussed in Gölles et al. (2014) and Seeber et al. (2019), and extended by appropriate terms to fulfill specific process behavior apparent from open-loop experiments. For the sake of brevity, the state space representation of the resulting grey-box model is abbreviated by the nonlinear vector-valued state function $\boldsymbol{f}$ and output function $\boldsymbol{g}$, see Eq. (1), where $\boldsymbol{x}$ is the state vector, $\boldsymbol{u}_m^T = [m^{\cdot}_{fuel,1}, m^{\cdot}_{pa}, m^{\cdot}_{sa,1}, m^{\cdot}_{sa,2}]$ the input vector, $\boldsymbol{\theta}$ the vector of identified but a priori unknown model parameters, $\boldsymbol{p}$ the vector of fuel parameters, and $\boldsymbol{y}^T = [T_{sup}, O_2, T_{fb}]$ the output vector.

$$\begin{aligned} \dot{\boldsymbol{x}} &= \boldsymbol{f}(\boldsymbol{x}, \boldsymbol{u}_m, \boldsymbol{\theta}, \boldsymbol{p}) \\ \boldsymbol{y} &= \boldsymbol{g}(\boldsymbol{x}) \end{aligned} \qquad (1)$$

For a comprehensive insight into the equations, please see Böhler et al. (2020b). Since $\boldsymbol{p}$ comprises all fuel-related parameters, i.e. the upper calorific value H_u, the water content

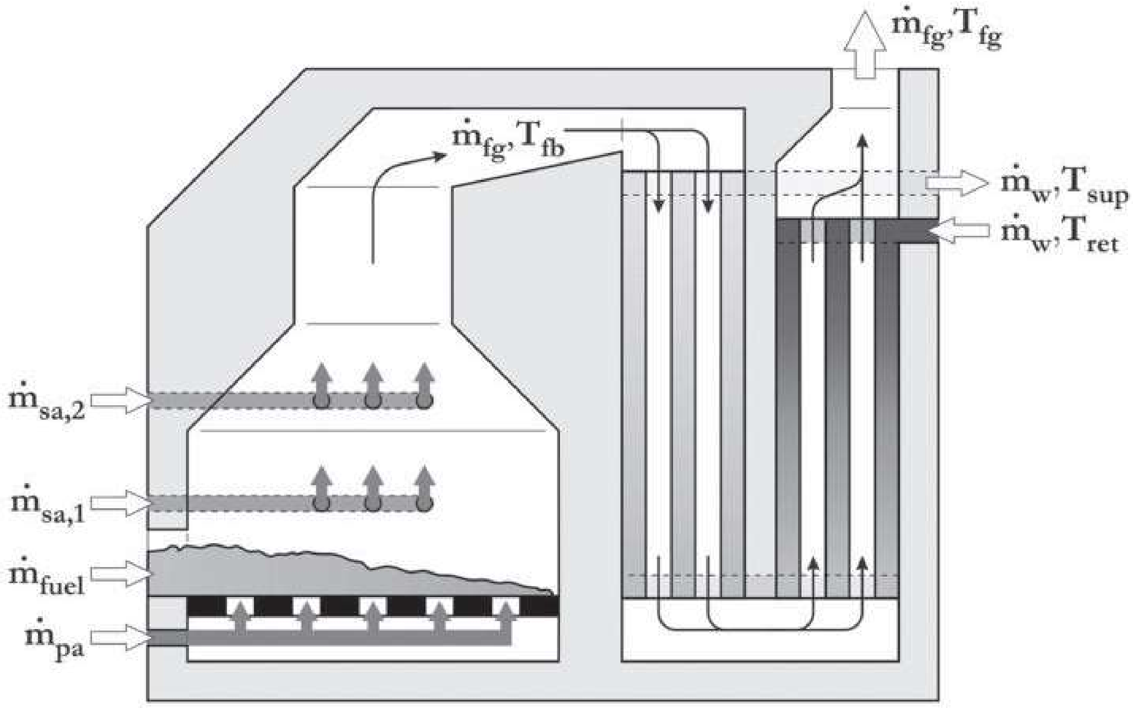

Fig. 1: Schematic illustration of the furnace with physical quantities essential for modelling.

w_{H_2O}, and ash content a_{ash}, the furnace model can be adapted to the combustion of other fuels in a simple and fast manner by updating related parameter values. Thus, the proposed modelling approach enables an advanced model-based control design inherently capable of handling fuel switches without extensive additional system identification.

In view of high combustion efficiency and emission reduction, formation of carbon monoxide (CO) is of particular interest. Böhler et al. (2019) developed a CO formation model, based on a neural network, for the combustion of wooden pellets using the very same furnace investigated here and thereby found a static dependency of CO on O_2 and T_{fb} to be appropriate, see Fig. 2a. Due to its highly nonlinear nature, a linear control approach with direct incorporation of the formation process lacks of desired performance. However, a closer analysis of the CO map unveils a simple emission limiting operating strategy to improve performance and simultaneously keep complexity

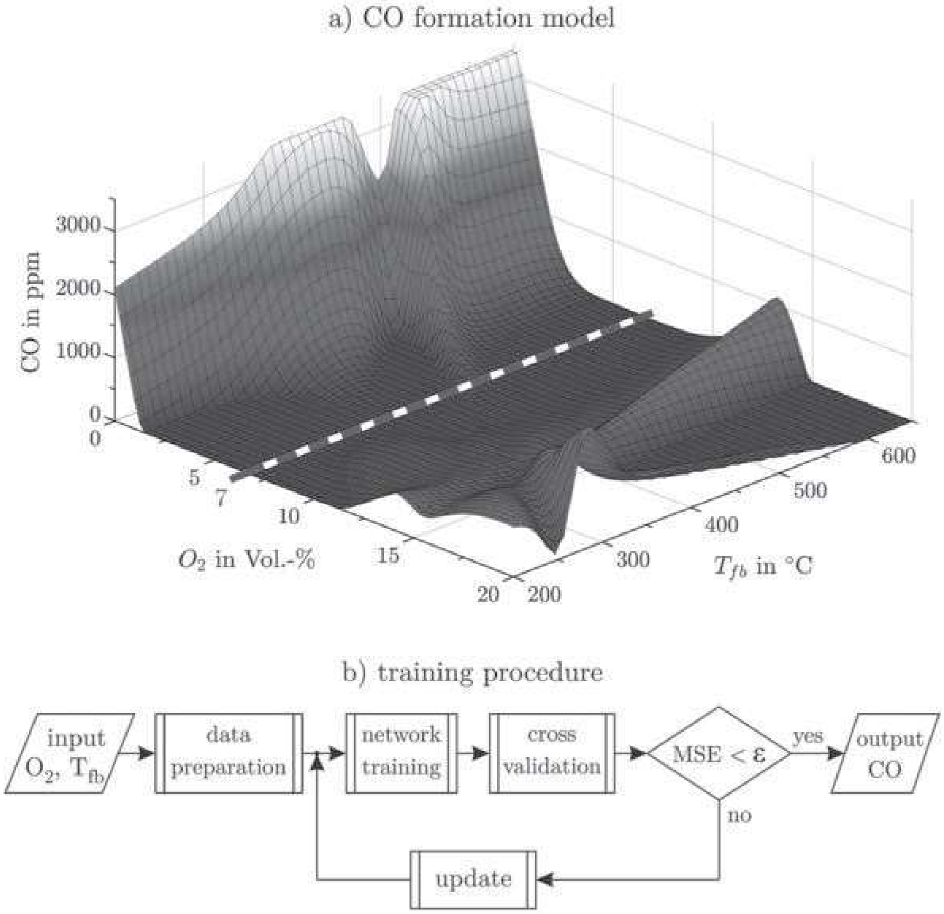

Fig. 2: In (a) a graphical representation of the utilized CO emission model for the combustion of wooden pellets is depicted. Besides the dependency of CO emissions on the oxygen concentration O_2 and freeboard temperature T_{fb}, a suboptimal but simple O_2 reference value for low CO emissions, indicated by the dashed line at 7 Vol.-%, is shown. Please note that the sharp limit at 3500 ppm indicates sensor saturation. The general training procedure (b) for the CO estimation model essentially consists of training, validation, and update in a loop until a performance criterion is met, e.g. mean squared error MSE falls below a certain value ε.

at bay. A constant oxygen concentration of 7 Vol.-% within the whole operating range fulfills these requirements for the combustion of wooden pellets, see line in the CO map (Fig. 2a) and results based on this strategy presented in **Section 4.** As measurements of O_2, T_{fb}, and CO are available in most furnaces, similar formation maps could be generated for other furnaces as well as fuels. The general training procedure, see Fig. 2b, comprises data preparation and identification in the loop until a predefined performance criterion is fulfilled. Detailed information is presented in Böhler et al. (2019).

3. CONTROLLER DESIGN

The conceptual architecture of the overall control structure (Fig. 3) is reasonably divided into the extended furnace, comprising immutable units established by the furnace manufacturer, and the extended controller, for which its design is discussed within this section.

Since application of simple PI control loops is common for control of small-scale biomass furnaces (Kaltschmidt et al. 2016), satisfying performance, related to such an approach, calls for decoupling and linear input-output behavior of the process under consideration. Therefore, the manufacturer intended the input interface to bridge the gap between these generally not compatible demands. Its implementation together with the actuator dynamics is described by the mapping $[\boldsymbol{T}_{sup,ref}(k), \boldsymbol{u}^T(k)] \mapsto \boldsymbol{u}_m^T$. Based on empirically evolved knowledge in the form of static look-up tables, the feedforward controller determines input values $\boldsymbol{u}_{ff}$ subject to the supply temperature reference $\boldsymbol{T}_{sup,ref}$

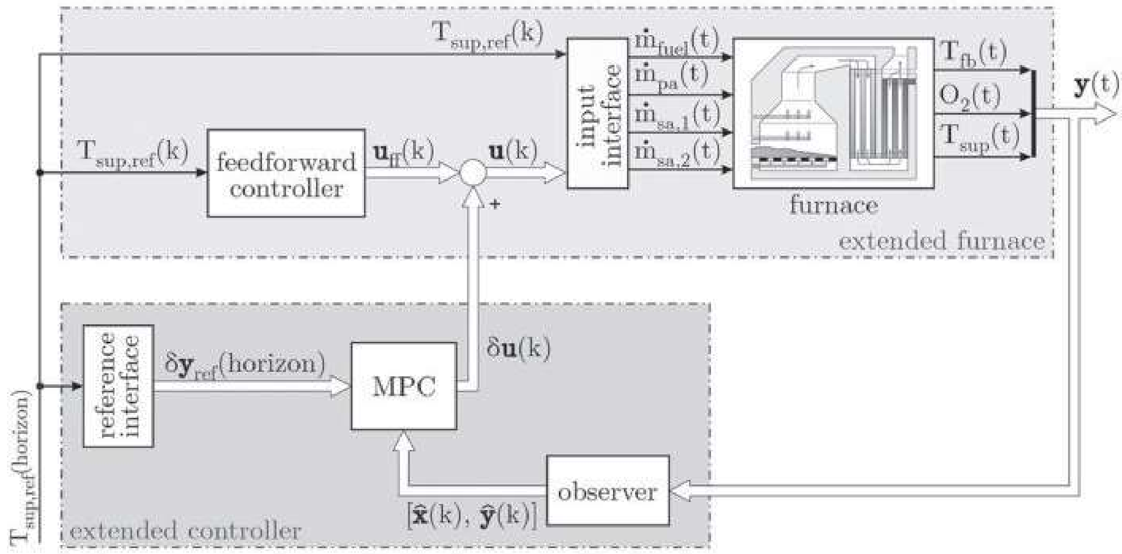

Fig. 3: Conceptual architecture of the overall control structure. While the presented furnace, its input interface, and feedforward controller together constitute the extended furnace, the extended controller comprises an MPC, a state observer, and an interface calculating necessary reference values.

and the currently used fuel in order to allow for high combustion quality during undisturbed steady-state operation. However, not only missing disturbance rejection but also the solely static implementation calls for a feedback-based and deviation-related control action δu yielding total control input $\boldsymbol{u} = \boldsymbol{u}_{ff} + \delta\boldsymbol{u}$.

In this work a linear MPC is established to fulfill this requirement. Therefore, a linearized model of the furnace together with the input interface is needed. Out of the large set of steady state operating points the, ν-gap metric, introduced by Vinnicombe (2001) and utilized by Böhler et al. (2020a) for a similar purpose, provides a useful framework to determine a linearization point in a methodically correct manner. Comparison of different linear models concerning their ability to be controlled by a single linear controller reveals an optimal linearization point robust in the face of changing the operating point. Based on the so defined linearized model, the basic MPC formulation (Wang 2009) is appropriately adapted to fit the specific needs. The conclusive optimization problem is given by Eq. (2) subject to the dynamics of the linearized system and constraints according to Eqs. (3), whereby J is the cost function, $\boldsymbol{\Delta U}$ is the vector of stacked incremental inputs within the horizon, $\boldsymbol{Y}$ and $\boldsymbol{Y}_{ref}$ are the vector of stacked outputs and output references, respectively, and $\boldsymbol{R}$ and $\boldsymbol{Q}$ are weighting matrices.

$$\Delta \boldsymbol{U}^* = \arg\min_{\Delta \boldsymbol{U},s}\{J\} = \arg\min_{\Delta \boldsymbol{U},s}\left\{\Delta \boldsymbol{U}^T \boldsymbol{R}\, \Delta \boldsymbol{U} + \left(\boldsymbol{Y}_{ref} - \boldsymbol{Y}\right)^T \boldsymbol{Q}\left(\boldsymbol{Y}_{ref} - \boldsymbol{Y}\right) + J_{sc}(s)\right\} \quad \textbf{(2)}$$

$$\boldsymbol{u}_{min} \le \boldsymbol{u}(k) \le \boldsymbol{u}_{max} \quad \forall k \in horizon \quad \textbf{(3a)}$$

$$O_{2,min} - s \le O_2(k) \quad \forall k \in horizon \quad \textbf{(3b)}$$

While real actuator limits (lower bound $\boldsymbol{u}_{min}$, upper bound $\boldsymbol{u}_{max}$) require input constraints, see Eq. (3a), to be incorporated as hard limits, hard output constraints could drive the problem infeasible. To overcome this issue, relevant lower oxygen limit $O_{2,min}$ is softened by introducing a so-called slack variable s, see Eq. (3b). Related cost term $J_{sc}(s)=c_1\, s+c_2 s^2$ enables tuning of soft constraint's strength by appropriately adapting positive real-valued constants c_1 and c_2. According to the receding horizon principle, only the first element of $\boldsymbol{\Delta U}^*$, the solution found by optimization, is utilized to form the actual control input.

To overcome lack of full state measurability, an extended Kalman filter, see e.g. Haykin (2004), provides estimates of the model states $\hat{\boldsymbol{x}}$ and outputs $\hat{\boldsymbol{y}}$. Due to the separation principle, the observer is designed independently of the controller, based on actual open-loop plant behavior.

Since the desired supply temperature represents the primary objective, the reference interface additionally provides reference values for O_2 and T_{fb}. To account for the deviation-related controller setup, absolute reference values $\boldsymbol{y}_{ref}$ are related to output values $\boldsymbol{y}_{ff}$ gained by only applying feedforward control action, therefore providing $\delta\boldsymbol{y}_{ref} = \boldsymbol{y}_{ref} - \boldsymbol{y}_{ff}$ to the MPC.

4. RESULTS AND DISCUSSION

Experimental results of the closed-loop introduced in **Section 3** are presented in Fig. 4 for the combustion of different solid biofuels. While all MPC configurations rely on a prediction horizon of 30 min and a control horizon of 15 min, weighting matrices are slightly adapted from experiment to experiment to serve specific fuel characteristics (Böhler et al. 2020b). Although the supply temperature reference profile - as the fundamental user input - covers the whole operating range in all experiments, strategies differ in the applied oxygen reference related thereto. While combustion control of wooden pellets (Fig. 4a) and olive stones (Fig. 4b) consider introduced emission limiting control strategy, combustion of wood chips (Figs. 4c and 4d) is carried out based on (slightly adapted) oxygen references provided by the feedforward controller.

In view of wooden pellets, comparison of CO emissions (subplot indicated by ★ in Fig. 4a) associated with proposed operating strategy (solid line) and averaged emissions related to conventional mode (dashed line) clearly underpins the beneficial use of oxygen references based on emission models. Overall improvement is additionally apparent by a decrease of the total average value from 99 to 24 ppm.

Besides emission reduction, fuel flexibility as wells as a simple way of handling fuel switches is highly valuable as not considered in any previous work on biomass furnaces. Fuel analysis supplies sufficiently accurate parameter values to appropriately adapt the furnace model and, based on that, the MPC matrices. Fig. 4b-d depict experimental results for combustion of olive stones and wood chips with two different water contents, for which fuel switches were handled with the MPC approach. Measurement data clearly indicate high robustness in the presence of fuel-related modifications.

Even though the proposed MPC scheme provides comprehensive advantages, its performance is mainly limited by given add-ons kept very simple in their design. Therefore, a complete model-based redesign of the overall control setup seems to enable extensive improvements. Substantial enhancement would come along with replacing the static feedforward controller by a dynamic (and nonlinear) one. Since then the feedback control law only has to cover perturbation rejection. With this in mind, a standard state feedback control is likely to perform as well as the proposed sophisticated model predictive approach. Associated simplicity of the overall control architecture would immensely decrease application barriers.

5. CONCLUSIONS

Presented control strategy for small-scale biomass furnaces enhances basic advantages of a model predictive approach by emission limiting oxygen references and a model-based framework to handle fuel switches in an efficient way. Maintaining overall performance while simplifying system complexity could be achieved by comprehensive redesign of the feedforward path, driving it a promising concept for broader application.

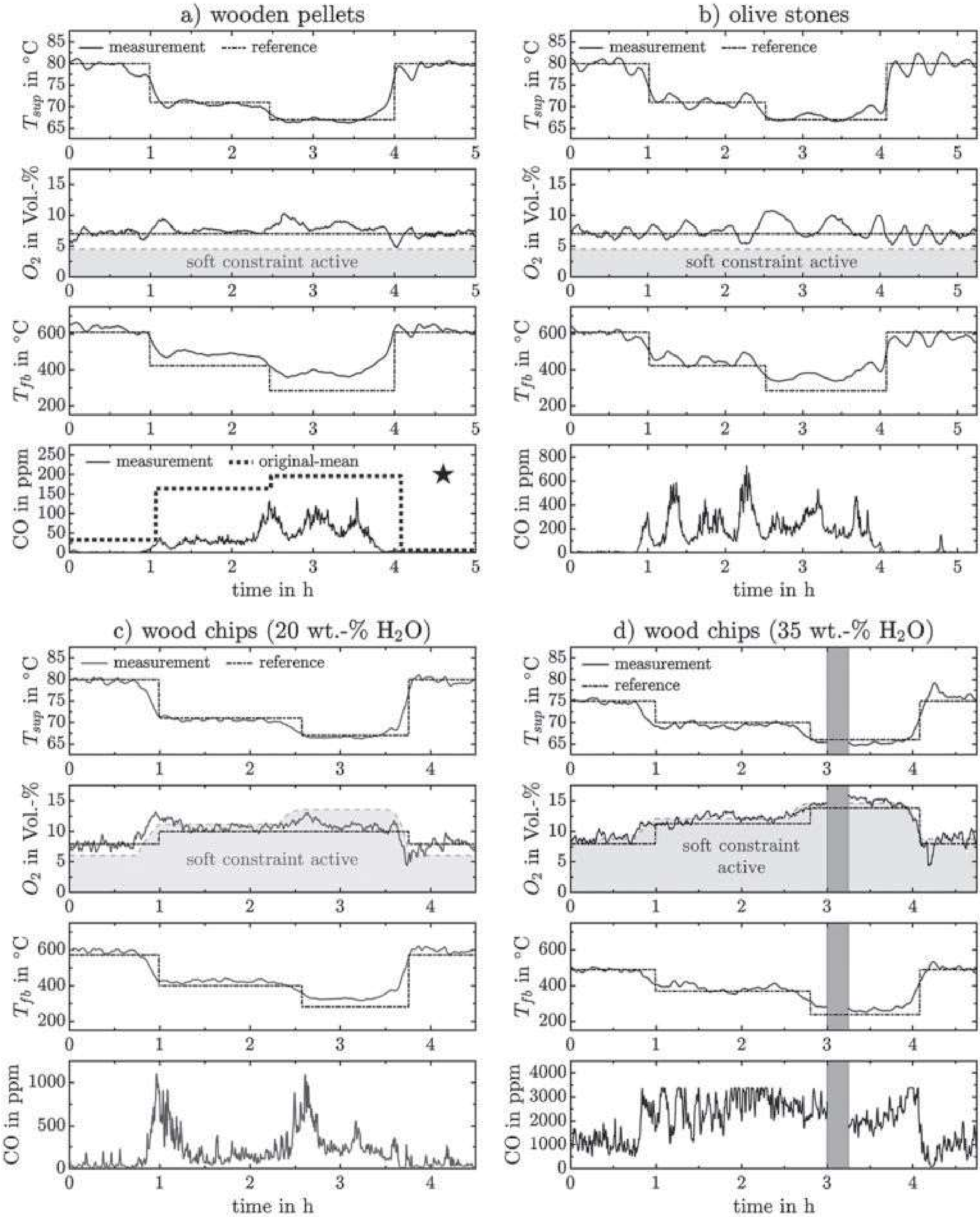

Fig. 4: Experimental closed-loop output results obtained by utilizing introduced controller design for combustion of different solid biofuels. Output results and measured CO emissions for the combustion of (a) wooden pellets and (b) olive stones are obtained by introducing emission limiting control settings. While results for the combustion of wood chips with a water content of (c) 20wt.-% are based on slightly adapted O_2 references, those for wood chips with a water content of (d) 35wt.-% rely on references supplied by the feedforward controller only. Shaded background highlights O_2 value ranges that cause additional costs due to violation of the implemented soft constraint. Vertical areas in (d) indicate interruption due to automatic furnace cleaning.

6. ACKNOWLEDGMENTS

The continuing support and the supply with test data of the furnace by FH-Burgenland, Herz Energietechnik GmbH, and Binder Energietechnik GmbH are gratefully acknowledged. This project (#853.606) is funded by the Climate and Energy Fund and conducted under the 2015 Energy Research Program.

REFERENCE

Böhler L., Görtler G., Krail J., and Kozek M. (2019) Carbon monoxide emission models for small-scale biomass combustion of wooden pellets. Applied Energy 254, 113668.

Böhler L., Krail J., Görtler G., and Kozek M. (2020a) Fuzzy model predictive control for small-scale biomass combustion furnaces. Applied Energy 276, 115339.

Böhler L., Fallmann M., Görtler G., Krail J., Schittl F., and Kozek M. (2020b) Emission Limited Model Predictive Control of a Small-Scale Biomass Furnace. Applied Energy (submitted).

Gölles M., Reiter S., Brunner T., Dourdoumas N., and Obernberger I. (2014) Model based control of a small-scale biomass boiler. Control Engineering Practice 22, 94-102.

Haykin S. (2004) Kalman filtering and neural networks. United States of America: John Wiley & Sons.

Kaltschmidt M., Hartmann H., and Hofbauer H. (2016) Energie aus Biomasse: Grund-lagen, Techniken und Verfahren. Germany: Springer-Verlag Berlin-Heidelberg.

Korpela T. M., Björkqvist T. K., Lautala P. A. (2009) Control strategy for small-scale wood chip combustion. IFAC Proceedings Volumes 42, 119-124.

Kortela J., Jämsä-Jounela S.-L. (2014) Model predictive control utilizing fuel and moisture soft-sensors for the biopower 5 combined heat and power (chp) plant. Applied Energy 131, 189-200.

Peng H., Ozaki T., Toyoda Y., Shioya H., Nakano K., Haggan-Ozaki V., Mori M. (2004) RBF-ARX model-based nonlinear system modeling and predictive control with application to a NOx decomposition process. Control Engineering Practice 12, 191-203.

Seeber R., Gölles M., Dourdoumas N., and Horn M. (2019) Reference shaping for model-based control of biomass grate boilers. Control Engineering Practice 82, 173-184.

Vinnicombe G. (2001) Uncertainty and Feedback: H(infinity) Loop-shaping and the (nu)-gap Metric. Great Britain: Imperial College Press.

Wang L. (2009) Model Predictive Control System Design and Implementation Using MATLAB®. Great Britain: Springer-Verlag London Limited.

Contact:
Markus Fallmann,
TU Wien, Getreidemarkt 9/E325,
1060 Wien, Austria,
Tel.: +43 (1) 58801 325523,
Email: markus.fallmann@tuwien.ac.at